Technical Article

Automated Ultrasound Measurement of the Inferior Vena Cava: An Animal Study

Ultrasonic Imaging
2020, Vol. 42(3) 148–158

DOI: 10.1177/0161734620912345
journals.sagepub.com/home/uix
SAGE

Jiangang Chen[1]*, Jiawei Li[2]*, Xin Ding[3], Gaofeng Wei[4], Xiaoting Wang[3], and Qingli Li[1]

Abstract

Because of continuous movement and variation in diameter of the inferior vena cava (IVC) with respiration, the measurements on IVC are labor-intensive and with considerable inter-operator variations. Some computer-assisted techniques have been developed to track the movement of the IVC semi-automatically. However, existing methods predominantly rely on reference marker selection and require many manual inputs. In this study, we developed a cross-correlation (CC)-based method for automated IVC movement tracking and measurement, which requires minimal manual input and avoids manual selection of reference markers. Based on the CC method, two approaches, named direct and relative approaches, were used to calculate the maximum, minimum, and variation of the IVC diameter, and compared with the manual measurement. Fifty-four ultrasound cine-loops collected from nine pigs were tested. The results reveal that both the proposed approaches were well agreed with the manual measurement. The errors of the direct approach were less than 9%, while those of relative approach were as high as 26.7%. It is concluded that the proposed direct approach is superior for IVC diameter measurements, which can be comparable with manual counterpart, serving as an alternative to traditional IVC measurement.

Keywords

ultrasound, vessel identification, vessel localization, inferior vena cava, automated measurement

Introduction

Because of its time- and cost-efficiency, ultrasonography has been increasingly used to measure the inferior vena cava (IVC) as a bedside point-of-care method for clinicians, especially for those in the Emergency Department and Intensive Care Unit, to quickly and conveniently measure a patient's status.[1-3] Ultrasound measurements on the diameter variation of the IVC during respiration can provide timely information on volume status in various patients, including healthy children,[4] healthy blood donors,[5] critically ill patients,[6] and those with liver fibrosis or cirrhosis.[7] In addition, dynamic parameters of IVC measured by ultrasound can clinically support fluid responsiveness determination and guide fluid therapy for critically ill, ventilated patients.[8-11]

However, ultrasound IVC measurements can be affected by the fact that the IVC is continuously moving with respiration. First, the measurement of a moving IVC is labor-intensive, time-consuming and clinician-dependent.[6] To measure the IVC diameter, a clinician must fix the ultrasound probe with one hand and operate on the ultrasound equipment with the other hand; or alternatively, make the measurement offline. Second, such measurements lead to significant inter-operator variability, making the measurements less standardized.[12] Third, longitudinal and cross-sectional screening methods further contribute to variable diagnostic cutoffs in the clinical practice.[13]

On the contrary, to make the ultrasound measurements with less operator dependence and better inter-operator agreement, a variety of smart algorithms have been developed for automated ultrasound measurement for different parameters, for example, vessel diameter and wall thickness.[14-18] Regarding the measurement of the IVC diameter using ultrasound, computer-assisted technologies have been developed

[1]Shanghai Key Laboratory of Multidimensional Information Processing, East China Normal University, Shanghai, China
[2]Department of Medical Ultrasound, Fudan University Shanghai Cancer Center, and Department of Oncology, Shanghai Medical College, Fudan University, Shanghai, China
[3]Department of Critical Care Medicine, Peking Union Medical College Hospital, Peking Union Medical College, Chinese Academy of Medical Sciences, Beijing, China
[4]Naval Medical Department, Naval Medical University, Shanghai, China

*These authors contributed equally.

Corresponding Author:
Qingli Li, Shanghai Key Laboratory of Multidimensional Information Processing, East China Normal University, #500 Dongchuan Rd., Shanghai 200241, China.
Email: qlli@cs.ecnu.edu.cn

Table 1. Information of Pigs Tested in the Study.

	Pig 1	Pig 2	Pig 3	Pig 4	Pig 5	Pig 6	Pig 7	Pig 8	Pig 9
Gender	F	F	F	F	F	F	F	F	F
Weight (kg)	28.8	34.8	33.3	37.4	34	30	36	26.9	30
Age (week)	13	16	15	16	15	14	16	13	14

for both longitudinal and transverse measurements.[19-22] Using longitudinal scanning, Mesin et al.[19] proposed a semi-automated approach in which the operator was required to first place two reference markers as a base for future movement and rotation tracking, and then use two more points to indicate a moving M-line. The diameter of the IVC was measured along the moving M-line in a frame. The movement and rotation of the IVC is followed by tracking the movement of two reference points, which kept a constant angle to the moving M-line. However, this method relies heavily on the selection of reference markers for the reference points, reducing its robustness. Bellows et al.[21] proposed an image processing method to track the respiratory movement and measure the diameter of the IVC under transverse scanning. A modified watershed approach was applied to extract the IVC from the background based on a seed manually placed in the IVC region. The algorithm was implemented recursively along the time step to achieve final measurements. However, in this approach, the IVC could easily be lost during respiration, resulting in anguish for the clinicians while the video clip must be paused and manual re-initialization is required to finalize the process.

Although these methods reduced some repetitive work of the doctors, they either require careful selection of reference markers or many manual inputs during initialization and multiple interactions for re-initialization, making them less reliable and susceptible to human errors.

Being aware of these drawbacks, in this study, we developed an automated method for IVC movement tracking and diameter measurement using normalized cross-correlation (NCC) techniques, which require minimal reference marker selections and manual inputs. The purpose of the study was to evaluate the performance of the proposed automated approaches for IVC measurements with the manual measurement as the gold standard. The method was tested on ultrasound data collected from pigs.

Method

Two clinicians (both with >six years ultrasound experience) scanned nine pigs fed in pigsty (female, age: 13-16 weeks, Table 1) and collected ultrasound data using a clinically available ultrasound machine CX-50 (Philips Healthcare, Bothell, Washington) equipped with a curved array probe (C5-1, central frequency: 1-5 MHz). Three ultrasound cine-loops were collected from each pig by two clinicians following the subsequent protocol, resulting in 54

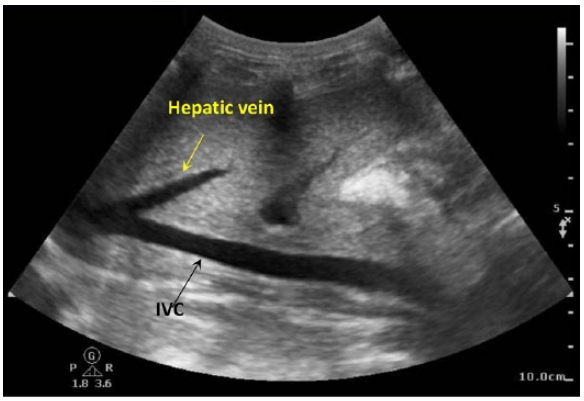

Figure 1. B-mode ultrasound images showing IVC and hepatic vein. IVC = inferior vena cava.

ultrasound data sets that were randomly sorted for the subsequent measurement. A laboratory developed algorithm using MATLAB (The MathWorks, Natick, Massachusetts) was applied to the collected ultrasound data for automated IVC movement tracking and diameter measurement. The automatically measured IVC diameters were compared with manual measurements by the two clinicians. The study was approved by the ethics committee of East China Normal University, Shanghai, China.

Experimental Protocol

1. The animal was fixed on the operation platform in the supine position.
2. The animal was pre-anesthetized with 846 mixture (0.8-1.0 mg/kg IM), then anesthesia was maintained by 3% to 4% isoflurane. The animal was mechanically ventilated at a volume calculated as volume = animal weight × 10 mL/kg at a rate of 26 to 32 breaths/min.
3. One clinician positioned the ultrasound transducer over the animal with the IVC shown on the center of the screen (Figure 1).
4. After the IVC was identified, the ultrasound transducer was fixed in position.
5. A cine-loop of 20 seconds (to cover at least three respiration cycles) in B-mode was collected under general abdominal imaging mode with the depth being 14 cm. The conversion of pixel to depth is achieved by dividing the depth by the height of the image for the automated approach.
6. The measurement site was then altered and steps (4) to (6) were repeated two more times.
7. Steps (4) to (7) were repeated by the other sonographer.
8. Data collected in DICOM format were stored in the ultrasound machine and then downloaded to a computer.

Before processing the data with the algorithm, the measurements on each data set were performed blindly and randomly by the two clinicians, including the maximum and minimum diameters of the IVC and IVC diameter variation (dIVC), which is calculated by

$$\mathrm{dIVC} = \frac{\varnothing_{\max} - \varnothing_{\min}}{\varnothing_{\max}}, \quad (1)$$

where $\varnothing_{\max}$ and $\varnothing_{\min}$ are the maximum and minimum diameter of the IVC, respectively.

Manual Measurement

Before performing the automated algorithm, the diameters of the IVC were manually measured on each frame of the collected cine-loops within one respiration cycle. The measurement was performed by placing two points on the upper and lower boundaries of the IVC at a position of 2 cm distal to the confluence of the hepatic vein.[19] The distance between the two points was set as the IVC diameter.

Automated Approach for IVC Movement Tracking and Diameter Measurement

Automated IVC localization and initial diameter measurement. Each of the collected cine-loops was denoised using a Gaussian low-pass filter with an 8×8 filter window. A seed point (denoted as P_0) was manually placed in the IVC region. Note that the manual placement of a seed point was to assure most of the cases were successful although it may be not necessary to place the seed point in a region of the vessel that has no other vessel branches. The proposed method did not require an exact location for the seed point. However, as the measurement of the IVC is suggested at a position of 2 cm distal to the confluence of the hepatic vein,[19] we developed the following process to exactly localize the measurement location automatically.

With P_0 as a starting point, the IVC was localized as follows:

i. With P_0 as the center, an annulus (inner diameter: 6 pixels, outer diameter: 14 pixels, width: 4 pixels) is created and growing up stepwise with the width kept constant. In each step, the standard deviation (*SD*) of the gray scales of the pixels in the annulus were computed and compared with the one in the previous step. The annulus stops growing when it touches the boundary of the vessel at some direction where the *SD* encounters a significant change (e.g., an increase of 50% in *SD*; Figure 2a). The annulus then shifts a little bit in the opposite direction. The above process is repeated until the annulus touches both the upper and lower boundaries of the IVC. At this moment, the center of the annulus is the central line of the IVC. The touching points of the annulus with the upper and lower boundaries of the IVC are denoted as P_u and P_l, respectively (Figure 2a). The outer diameter of the annulus is then equal to the diameter of the IVC at the current location.

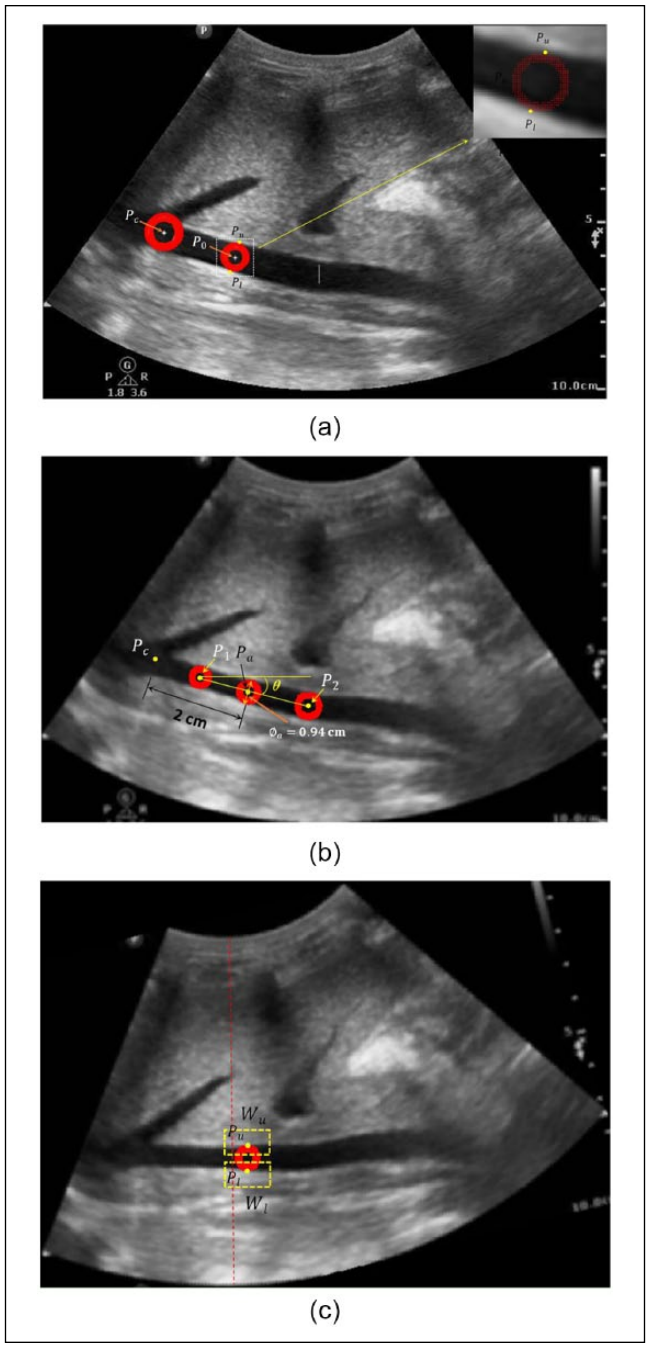

Figure 2. (a) IVC ultrasound image demonstrating the locations of the initial point manually placed (P_0) and the confluence of the hepatic vein (P_c). (b) IVC ultrasound image demonstrating the location 2 mm away from the confluence of the hepatic vein (P_a) and the two locations (P_1 and P_2) to get the angle of the IVC central line to the horizontal line. (c) IVC ultrasound image demonstrating two tracking window (W_u and W_L) for cross-correlation process. IVC = inferior vena cava.

ii. The circle moves longitudinally along the central line of the IVC toward the hepatic vein. All ultrasound scans followed the standard guideline, that is, the confluence of the hepatic vein is localized on the left side of the image.
iii. The movement stops when the circle reaches the confluence of the hepatic vein, under the conditions that
   a. The diameter of the circle increases significantly; for example, an increase of more than 30% in diameter;
   b. The circle has more than two touching points with the vessel boundaries. This is under the consideration that the confluence of the hepatic vein looks like a junction of three roads. The circle may touch three boundaries at the confluence (red circle with the center P_c; Figure 2a).
iv. With P_c as a reference, the IVC measurement location is automatically determined along the IVC central line; that is, 2 cm distal to the confluence of the hepatic vein (noted as P_a; Figure 2b). The IVC diameter was then determined and equal to the diameter of the circle at P_a, as denoted by $\varnothing_a$ in Figure 2(b).

Automated image rotation. To facilitate the NCC process, the image was rotated to keep the IVC horizontal. Such an operation was conducted automatically by the followed procedure:

1. The annulus moves leftward and rightward following the same rationale as the above described to position P_1 and P_2, respectively (Figure 2b). The locations of P_1 and P_2 were set 0.8 cm away from P_a, although this distance may need to vary if the algorithm is applied to different subjects, like humans.
2. The angle of the line $P_1 - P_2$ according to the x-axial is set to be θ (Figure 2b).
3. Apply the rotation algorithm in MATLAB to the processed image with the angle of θ, that is, "imrotate(imm, θ)," where imm is the image to be rotated. In the rotated image, the IVC is placed horizontally, as shown in Figure 2(c). Note that the red circle in Figure 2(c) is corresponding to the one centered at P_a in Figure 2(b), with P_u and P_l as the touching points with the upper and lower boundaries of the IVC, respectively.

Automated sampling window selection. With P_u and P_l as references, two rectangles embracing P_u and P_l, respectively, are automatically created (denoted as W_u and W_l; Figure 2c). W_u or W_l covers the IVC region (one-third height of the rectangle) and upper or lower IVC wall (two-thirds height of the rectangle), respectively. The sampling window selection is important for the following NCC algorithms. The ratio of the IVC region and IVC wall covered in the window is based on the consideration of (a) covering the IVC boundaries and (b) covering as much information as the IVC walls.

Automated movement tracking using NCC. The motion and diameter variation of the IVC are estimated by tracking the two-dimensional (2-D) movement of W_u and W_l using NCC.

First, consider a series of one-dimensional (1-D) signals that are the grayscale variations along a vertical line (e.g., red line in Figure 2c) in serial ultrasound frames. A pair of adjacent 1-D signals were selected for analysis, with one as the reference signal, the other as the comparison signal (Figure 3a). A portion of the reference or comparison signal was selected by a moving window. The signal within the window in reference and comparison signals are referred to as $f(n)$ and $g(n)$, respectively, where n is the sample index ($1 \le n \le M$, M is the total number of samples). The NCC coefficient of the reference and comparison windows, R_{NCC}, is defined as[13]

$$R_{\mathrm{NCC}} = \frac{\sum_{n=u}^{u+W-1} f(n)\, g(n+\tau)}{\sqrt{\sum_{n=u}^{u+W-1} f^2(n) \cdot \sum_{n=u}^{u+W-1} g^2(n+\tau)}}, \left(\tau_1 \le \tau \le \tau_2\right), \quad (2)$$

where the reference window is located within the interval of $[u, u + W - 1]$; u is the origin of the reference window, W is the window size, τ is the shift between the comparison and reference windows, and $[\tau_1, \tau_2]$ is the search range determined by the range of physiologic displacements.

The above-depicted 1-D kernel in a 1-D search for 1-D motion estimation can be extended to 2-D motions.[23] A detailed description of the NCC is beyond the scope of this paper, which can be referred to Luo and Konofagou.[24] Applying the NCC, the dynamic movements of W_u and W_l in 2-D directions can be traced, with the coordinates of W_u and W_l at each frame serving as the reference for the following IVC diameter measurements. Figure 3(b) demonstrates the movement tracking at an intermediate frame.

Automated measurement of dynamic change of IVC diameter. With the locations of W_u and W_l at every frame achieved by the above-described NCC algorithm, two approaches, named as relative approach and direct approach, were applied to calculate the IVC diameter, which continuously changes with respiration.

Relative approach. In the relative approach, the IVC diameter at the first frame (i.e., $n = 1$, denoted as $\varnothing_1$) of a cine-loop was measured using the above-described annulus method, serving as a basis for further processes. The IVC diameters in the subsequent frames ($\varnothing_n, n > 1$) were then calculated by accumulatively superposing the displacements of W_u and W_l in the vertical direction (denoted as δ_k^u and δ_k^l, respectively) to $\varnothing_1$, that is,

$$\varnothing_n = \varnothing_1 + \sum_{k=2}^{n} \left(\delta_k^u - \delta_k^l\right),\ k = 2,3,\ldots \quad (3)$$

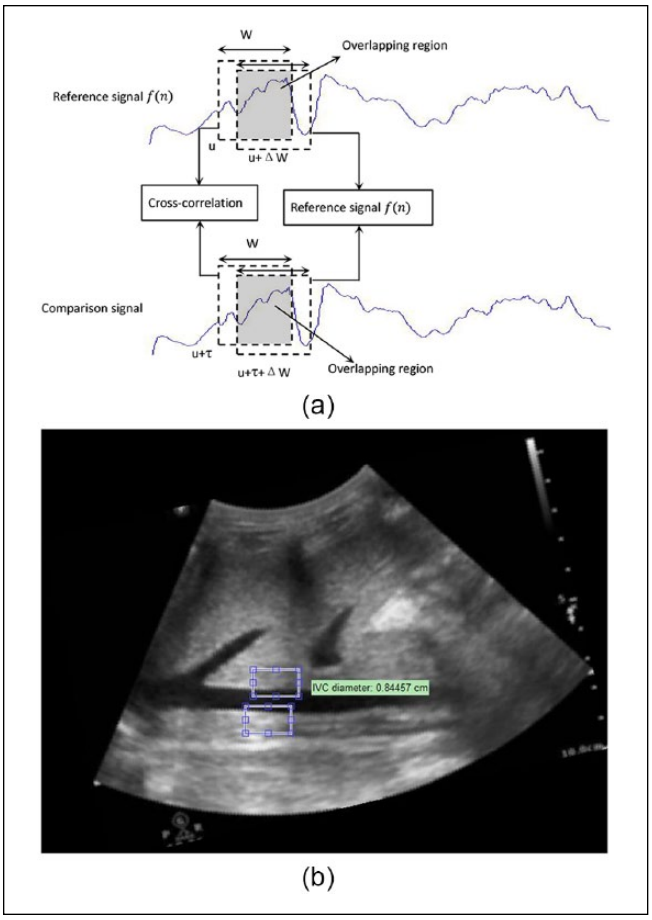

Figure 3. (a) A schematic diagram of redundant calculations of the non-normalized cross-correlation between the reference and comparison windows. The overlapping regions (i.e., redundant calculations) were indicated by the gray areas. (b) An intermediate frame demonstrating the movement tracking.

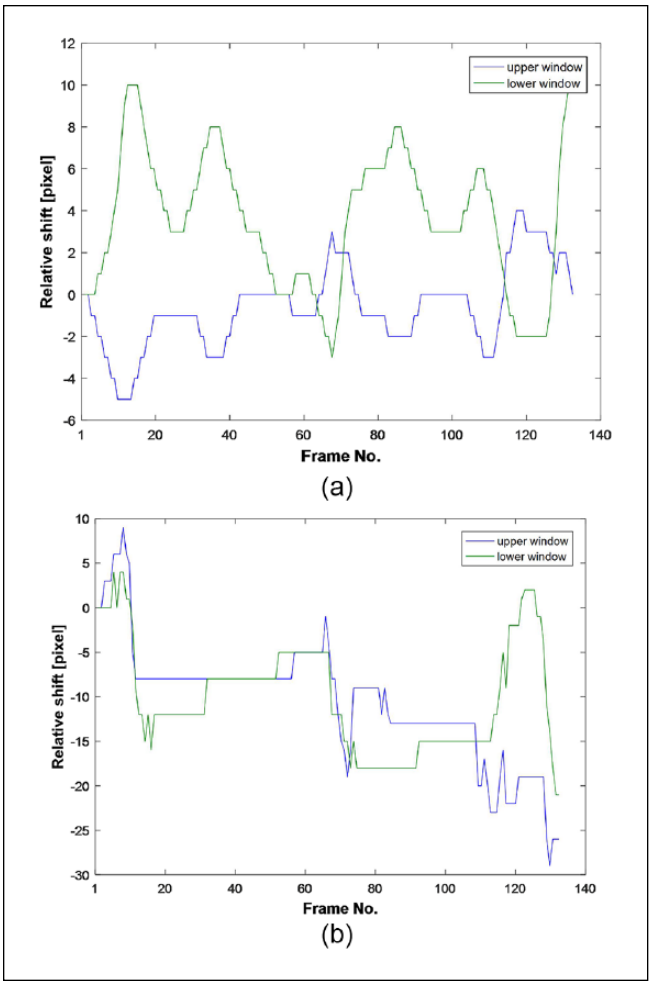

Figure 4. Displacement tracks of the tracking windows in the (a) vertical and (b) horizontal directions. For interpretation of the references to colours in this figure legend, refer to the online version of this article.

$$\delta_k^u = y_k^u - y_{k-1}^u,\ k = 2,3,\ldots \tag{4}$$

$$\delta_k^l = y_k^l - y_{k-1}^l,\ k = 2,3,\ldots \tag{5}$$

where $\varnothing_n$ is the IVC diameter at the frame n; y_k^u and y_k^l are the coordinates of the center of W_u and W_l in the vertical direction at frame k, respectively; k is an operator that denotes a frame prior to the frame n. The displacement tracks of W_u and W_l in the vertical direction are presented in Figure 4(a). In the plot, the movement direction of the window toward the transducer is defined as positive; that away from the transducer is defined as negative.

Direct approach. In the direct approach, the IVC diameter is directly measured using the above-described annulus method at every frame of a cine-loop. The center of the annulus is dynamically determined based on the locations of both W_u and W_l in the horizontal direction; that is,

$$C_n^x = \frac{1}{2}\left(x_n^u + x_n^l\right),\ n = 1,2,\ldots \tag{6}$$

$$C_n^y = \frac{1}{2}\left(y_n^u + y_n^l\right),\ n = 1,2,\ldots \tag{7}$$

where C_n^x and C_n^y are the coordinates of the center of the annulus in the horizontal and vertical directions at frame n, respectively; x_n^u and x_n^l are the coordinates of the center of W_u and W_l in the horizontal direction at frame n, respectively. The displacement tracks of W_u and W_l in the horizontal direction are presented in Figure 4(b). In the plot, the movement of the window rightward is defined as positive; that leftward is defined as negative.

Statistics

Statistical analyses were performed with SPSS for Windows version 22.0 (SPSS Inc., Chicago, Illinois). Diameters were presented as mean ± *SD*. Intra-class correlation coefficient (ICC) with 95% confidence interval (CI) was used to evaluate the reliability of inter-observer and intra-observer

measurements. Measurement errors between automated algorithms and manual method were compared with paired-samples t test. A two-tailed p value less than 0.05 was considered as statistically significant.

Results

Figure 4(a) and (b) shows the movement tracks of the centers of W_u and W_l referencing to the position in the first frame in horizontal and vertical directions, respectively. The effect of the tracking window size on the measurement was evaluated by comparing the automatically measured minimum/maximum diameter and dIVC with the manual counterparts with the tracking window varied from 20 to 50 pixels in height (the ratio of height to width is fixed to be 1:2), as shown in Figure 5(a) to (c), respectively. Figure 6 shows the diameter measured by the direct approach with the tracking window being 30 mm × 60 mm within two respiration cycles.

To validate the proposed method, the IVC diameters at every frame within one respiration cycle were measured using the direct, relative, and manual approaches. Note that the cine-loop of one respiration cycle for the measurement was randomly selected from the collected data sets which covered three respiration cycles as described above. Representatively, Figure 7(a) and (b) shows the IVC diameter measured using the three methods at every frame during one respiration cycle from one data set, and the measurement errors of the direct and relative methods compared with the manual method as the reference, respectively. The manually and automatically measured maximum and minimum diameters, as well as dIVC using the relative and direct approaches are compared in Figure 8.

The ICC for inter-observer measurement was 0.991 (95% CI: [0.986, 0.995]); the ICC for intra-observer measurement was 0.997 (95% CI: [0.995, 0.998]). The agreements of direct-manual and relative-manual were analyzed via Bland–Altman and plotted in Figure 9. Both the direct and relative methods agree with the manual method with all data points within the mean ± 1.96 *SD*. Table 2 summarizes measurement errors of the direct and relative methods with the manual method (gold standard). The errors of the direct approach are less than 9%, while those of relative approach are as high as 26.7%. The measurement error for the relative method was statistically larger than the direct method ($p < 0.0005$ for maximum diameter, minimum diameter, and dIVC).

Discussion

In this study, an automated method for IVC movement tracking and diameter measurement was developed using a cross-correlation algorithm. The whole process only requires the operator to roughly indicate the IVC by manually placing one seed in the IVC region. The method was tested on ultrasound cine-loops collected from nine pigs and validated by comparing with the manual measurements. Such a method

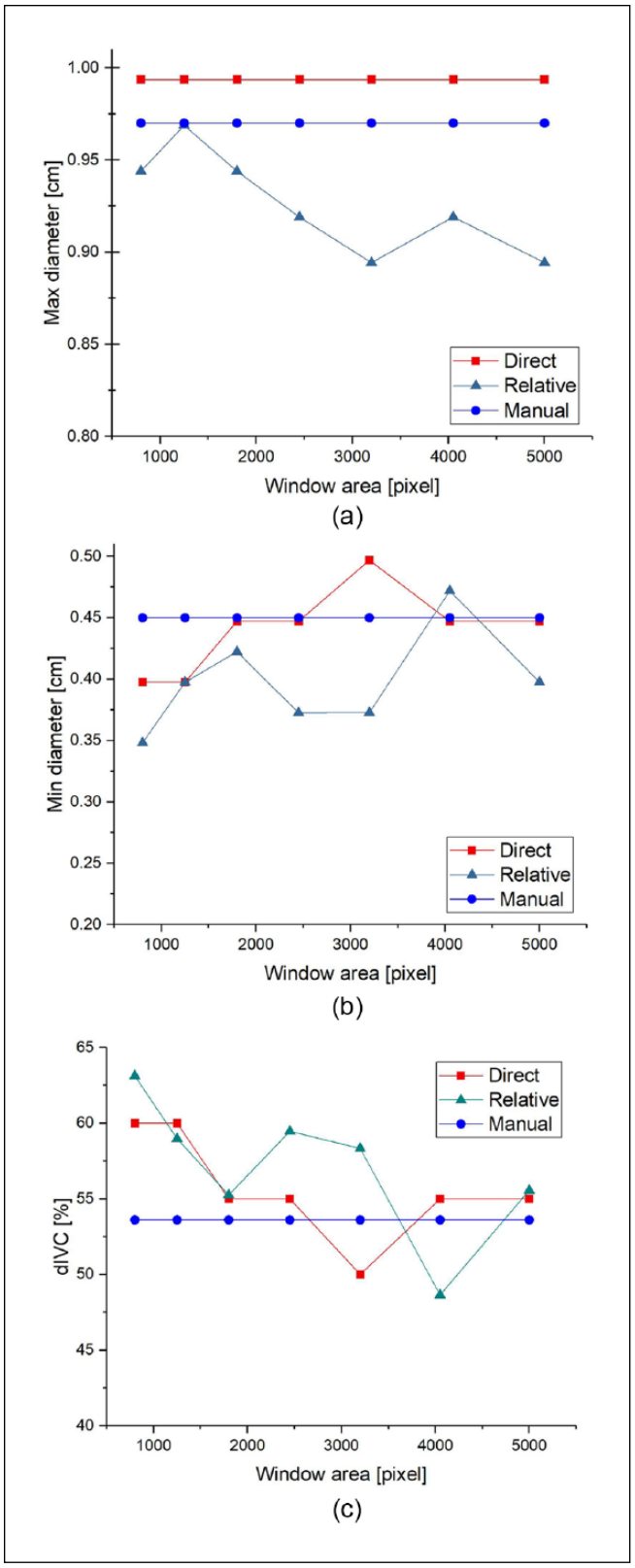

Figure 5. (a) Maximum diameter, (b) minimum diameter, and (c) dIVC measured by direct, relative, and manual approaches at different tracking window sizes from Pig 3. dIVC = IVC diameter variation.

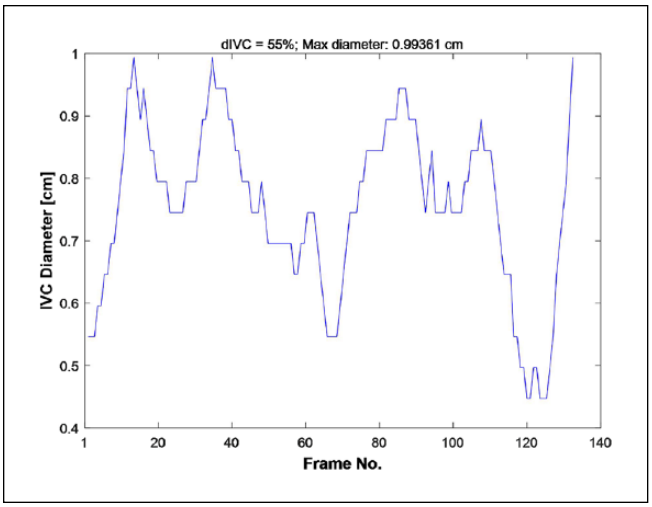

Figure 6. Variation of IVC diameter in two respiration cycles. IVC = inferior vena cava.

may reduce the need for repeated operations and improve the measurement accuracy, while the successful application of the proposed method relies on accurate ultrasound scans.

In the study, two tracking windows were automatically placed to cover the upper and lower vessel walls of the IVC, respectively, making our approach the least dependent on manual interventions. The pixels' gray values inside the window between adjacent frames were analyzed using Equation (2) to trace the displacement of the window using the cross-correlation algorithm. The displacements of the windows in the horizontal and vertical directions serve as the basis of the relative and direct approaches, respectively. Figure 4(a) and (b) shows the displacement of the upper and lower windows in vertical and horizontal directions, respectively. The upper and lower windows demonstrated opposite movement patterns in the vertical direction (Figure 4a), while similar movement patterns were seen in the horizontal direction (Figure 4b). Such an observation accords with the fact that both the upper and lower walls of the IVC move left and right synchronously, and upward and downward anti-synchronously during respiration.

The size of the rectangles for the NCC-based movement tracking may affect the measurement of the IVC diameter. To explore the effect of the tracking window size on the movement tracking and find the optimal trade-off, the automated algorithm for IVC measurement was tested with different tracking window sizes. Figure 5 shows the maximum and minimum diameter; the dIVC of Pig 3 obtained by the automated algorithm using the tracking window varied from 800 to 5000 pixels in area. By comparison, it was observed that the window size of 30 × 60 pixels was the optimal choice for the study because the maximum and minimum diameter, as well as the dIVC measured by the direct, relative, and manual methods, are closest at this window size. We thus chose this tracking window size to conduct the following experiments.

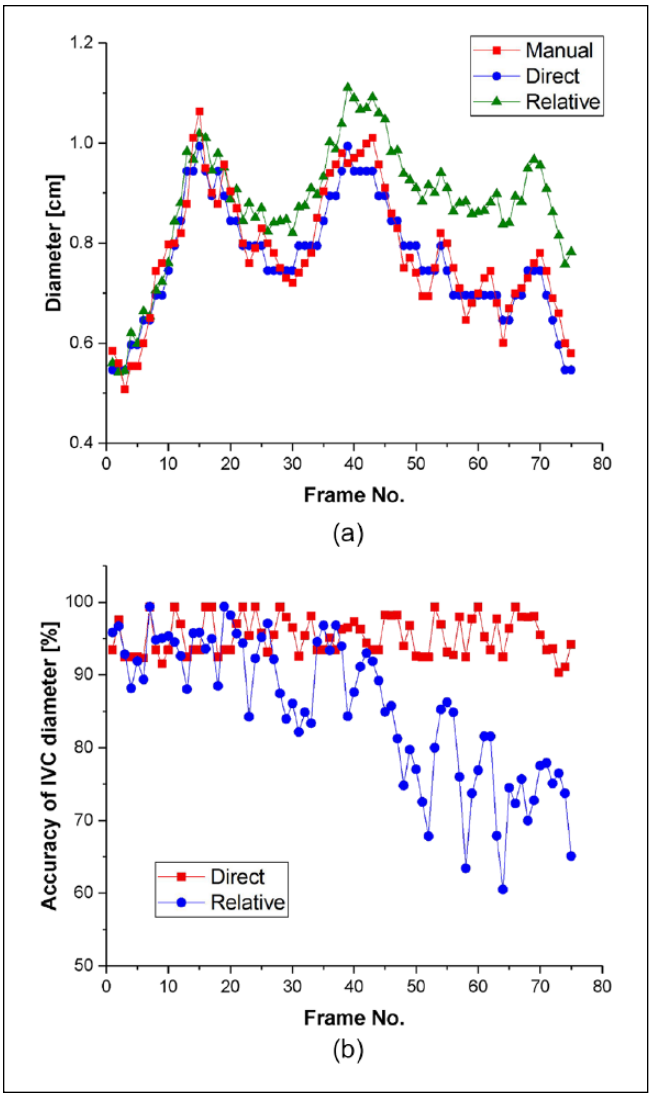

Figure 7. (a) The IVC diameter measured by the direct, relative, and manual methods at every frame during one respiration cycle from one data set and (b) the errors of the direct and relative methods with the manual measurement as reference. IVC = inferior vena cava.

In the study, two approaches were applied to calculate the IVC diameters: the relative method and direct method. The former calculates the IVC diameter by accumulating the relative frame-by-frame displacements of the tracking windows in the vertical direction to a base IVC diameter measured in the first frame; the latter directly measures the IVC diameter at every frame using the increasing annulus method with the measurement location (i.e., the center of the annulus) determined by the coordinates of both the upper and lower windows in the horizontal direction.

The diameters of the IVC at every frame measured by the direct, relative, and manual methods were compared in Figure 7(a). The IVC diameter measured by the direct approach matched well with that manually measured (errors

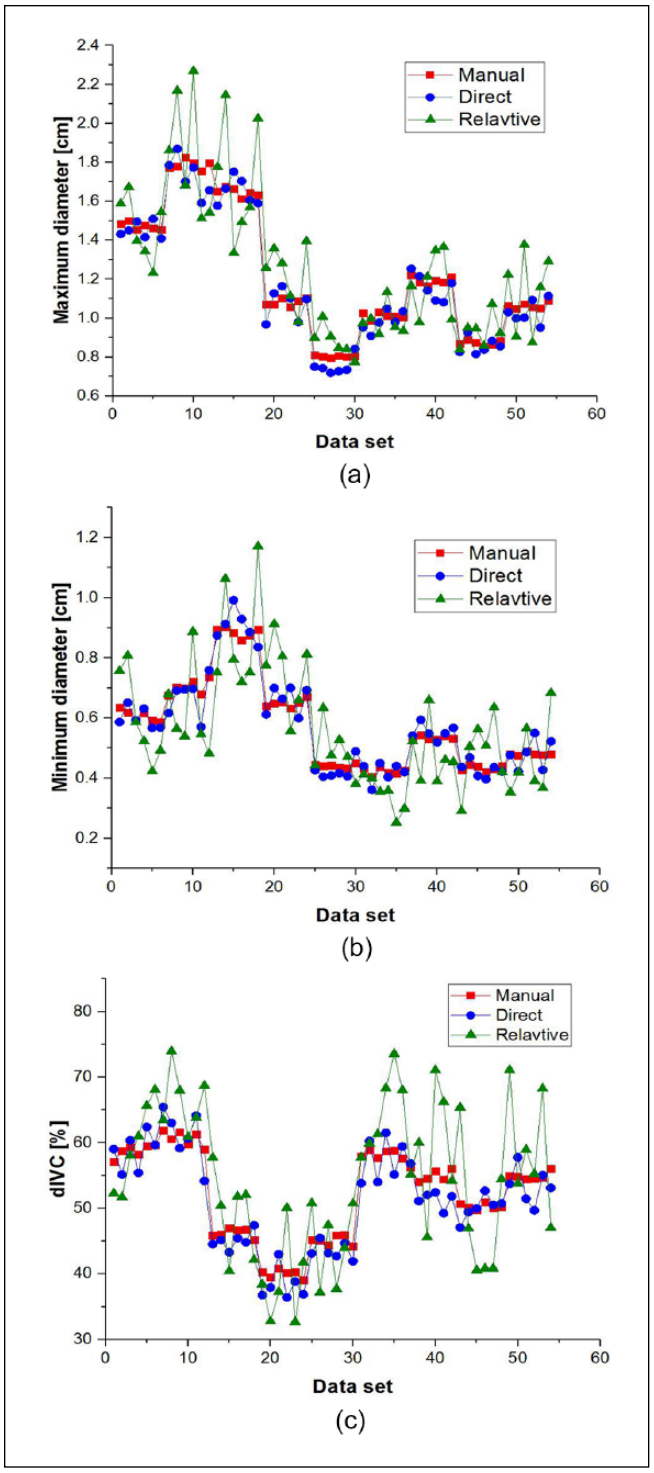

Figure 8. (a) Maximum diameter, (b) minimum diameter, and (c) dIVC measured from all the data sets by direct, relative, and manual approaches. dIVC = IVC diameter variation.

less than 9% as shown in Figure 7b). Meanwhile, the relative method showed larger deviations from the manual measurement than the direct method, in particular for the large frame numbers (errors larger than 30% for large frame

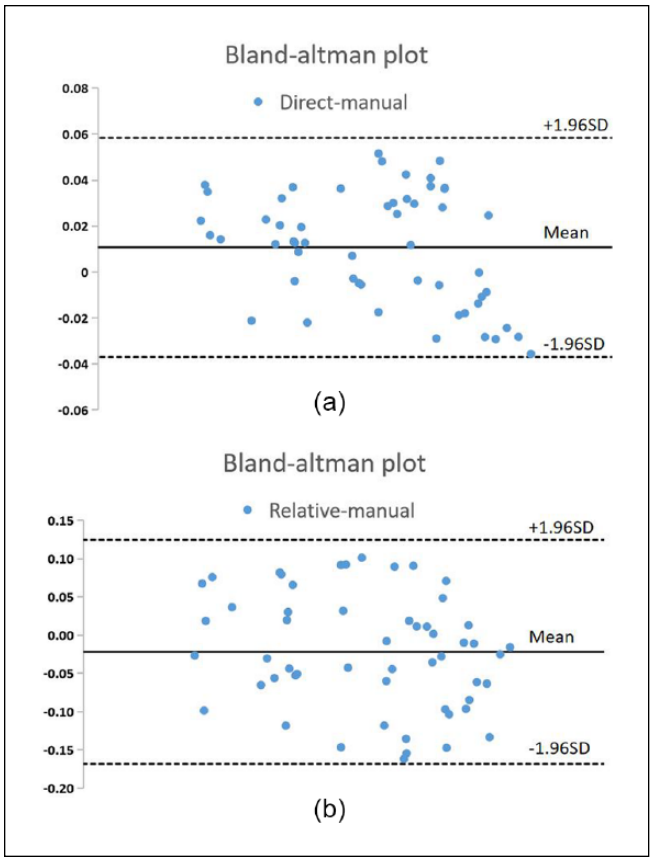

Figure 9. Bland–Altman plots of the (a) direct and (b) relative approaches referencing to the manual method.

numbers as shown in Figure 7b). Such a difference was additionally confirmed by the statistical analysis (Table 2) and the plot of final measurements of all data sets (Figure 8). In addition, the results obtained by the direct method were much more concurrent with the manual measurement than those of the relative method, as noticed from Figures 7(a) and 8. This can be explained by the fact that the diameter computed with the relative method is sensitive to accumulated error from the position of the tracking windows in previous frames. On the contrary, in the direct method, the diameter of the IVC is directly measured at each single frame; therefore, it is not affected by measurement bias or errors in the historical measurements. Thus, the direct approach outperforms the relative approach in the measurement of IVC, although both methods show agreement with the manual measurement, as illustrated in the Bland–Altman plot (Figure 9).

The proposed approach in this study offers an alternative option for automated IVC measurement to traditional methods, and outperforms existing counterparts in some aspects.

1. The proposed method requires the least manual inputs, meaning that only a single click is needed to indicate the IVC with the subsequent measurements

Table 2. Data on the Difference between the Automated Measurements (Direct Method and Relative Method) and Manual Measurement.

Measurement Error	Maximum Diameter (cm)	Minimum Diameter (cm)	dIVC (cm)
Direct vs. manual	0.057 ± 0.033	0.030 ± 0.024	0.023 ± 0.013
Relative vs. manual	0.154 ± 0.113	0.111 ± 0.067	0.064 ± 0.043
p value	<0.0005	<0.0005	<0.0005

Data are presented as mean ± *SD*. dIVC = IVC diameter variation.

processed automatically. Previous studies required many human interventions; for example, at least four manual inputs in the study by Mesin et al.[19] In the study by Bellows et al.,[21] a seed was manually placed in the IVC region at the beginning of the measurement. However, the subsequent IVC movement tracking and diameter measurement may further require multiple manual inputs for re-initialization when the algorithm fails to trace the IVC.

2. Despite the initial manual identification of the IVC, all the measurements on the maximum and minimum diameters, as well as the dIVC, were performed automatically by the algorithm. Most existing studies require manual measurement of the IVC diameter. In the study by Bellows et al.,[21] the IVC diameter had to be manually measured at the beginning of the method, which served as a basis for subsequent IVC measurements. This may introduce human errors.
3. There is not a high requirement for reference marker selection in our proposed approach. In this study, we used an NCC algorithm for the IVC movement tracking. The measurement location following the guideline was automatically selected. However, in the study by Mesin et al.,[19] two reference points were placed in or near reference markers (e.g., on the boundary of a vessel) to serve as a basis for movement tracking. This compromises the generalization of the application as the reference markers are not always clearly displayed in clinics.
4. The proposed diameter measurement approach using an increasing annulus in this study can guarantee that the measured diameter is the closest distance between the IVC boundaries, thus minimizing the errors if the IVC walls are not parallel in some pathological conditions. However, in the study by Mesin et al.,[19,20] the diameter of the IVC was calculated along a moving M-line that is being rotated following a fixed angle relative to the reference points during respiration. Such a manner may introduce measurement errors for the IVC diameter if (a) one side of the IVC is pushed resulting in non-parallel IVC boundaries or (b) the M-line is not perpendicular to the IVC walls because it is being rotated during the measurement.
5. The proposed NCC-based approach could be performed very fast and require a little computation resource to track motions from ultrasound cine-loops. It can be implemented on a scanner, like the mobile ultrasound, and performed in real time. On the contrary, most existing ultrasound automation studies were based on ultrasound images and utilized algorithms that require high computation capabilities, such as active contours and artificial neural networks.[14-18]

There are several limitations to the study. First, although the ultrasound data were collected by experienced clinicians and under good control, the IVC image quality was affected by a number of factors including body habitus, bowel gas, ultrasound artifact, the relative depth of the IVC in the body, and other factors, for example, gain, frame rate, depth of the machine and motions, and so on.[21] The image quality affects the ability of the automated algorithms to provide accurate results. Second, the algorithms were tested in animals. Humans may exhibit different anatomies in terms of depth, dimension, and movement pattern of the IVC, as well as the ultrasound image quality (e.g., contrast and noise). Third, the study was only conducted on healthy animals without any pathological conditions and under normal imaging conditions. In addition, the animals tested in the study were all under ventilation without natural breathing. Fourth, the study did not have a solid reference method as manual measurement was used as the gold standard.

Future study objectives will include (a) testing the automated algorithm on subjects under a variety of conditions (e.g., human subjects of different pathologies under natural breathing or ventilation, testing under compression such that the IVC displaces vertically in the image) with additional simulation and phantoms studies, (b) improving the algorithm to alleviate the influence of affecting factors on the IVC identification and localization (e.g., rib shadows), and (c) developing algorithms for IVC measurements using transverse scans.

Conclusion

In this study, we tested an NCC-based approach for automated IVC movement tracking and diameter measurement in pigs. Direct and relative automated approaches were applied

to calculate the IVC diameters varying with respiration, the relative and direct approaches. Our results showed that the direct approach was superior to the relative approach for the IVC diameter measurements. The proposed method not only provides an alternative way for automated IVC movement tracking and diameter measurement, but outperforms traditional methods in terms of less requirement on manual inputs and reference marker selections. Future studies will include improving the approach for human subjects with different pathological status and difficult cases.

Acknowledgments

The authors would like to thank the reviewers in advance for their comments and suggestions.

Declaration of Conflicting Interests

The author(s) declared no potential conflicts of interest with respect to the research, authorship, and/or publication of this article.

Funding

The author(s) disclosed receipt of the following financial support for the research, authorship, and/or publication of this article: This work was supported by the National Natural Science Foundation of China (Grant No. 61975056), the Shanghai Natural Science Foundation (Grant No. 19ZR1416000), and the Science and Technology Commission of Shanghai Municipality (Grant No. 14DZ2260800, 18511102500).

ORCID iD

Qingli Li https://orcid.org/0000-0001-5063-8801

References

1. Au AK, Matthew Fields J. Ultrasound measurement of inferior vena cava collapse predicts propofol-induced hypotension. Am J Emerg Med. 2017;35(3):508-9.
2. Finnerty NM, Panchal AR, Boulger C, Vira A, Bischof JJ, Amick C, et al. Inferior vena cava measurement with ultrasound: what is the best view and best mode. West J Emerg Med. 2017;18(3):496-501.
3. Gaskamp M, Blubaugh M, McCarthy LH, Scheid DC. Can bedside ultrasound inferior vena cava measurements accurately diagnose congestive heart failure in the emergency department? A clin-IQ. J Patient Cent Res Rev. 2016;3(4):230-4.
4. Haines EJ, Chiricolo GC, Aralica K, Briggs WM, Van Amerongen R, Laudenbach A, et al. Derivation of a pediatric growth curve for inferior vena caval diameter in healthy pediatric patients: brief report of initial curve development. Crit Ultrasound J. 2012;4(1):12.
5. Lyon M, Blaivas M, Brannam L. Sonographic measurement of the inferior vena cava as a marker of blood loss. Am J Emerg Med. 2005;23(1):45-50.
6. Akkaya A, Yesilaras M, Aksay E, Sever M, Atilla OD. The interrater reliability of ultrasound imaging of the inferior vena cava performed by emergency residents. Am J Emerg Med. 2013;31(10):1509-11.
7. Kitamura H, Kobayashi C. Impairment of change in diameter of the hepatic portion of the inferior vena cava: a sonographic sign of liver fibrosis or cirrhosis. J Ultrasound Med. 2005;24(3):355-9; quiz 360-1.
8. Machare-Delgado E, Decaro M, Marik PE. Inferior vena cava variation compared to pulse contour analysis as predictors of fluid responsiveness: a prospective cohort study. J Intensive Care Med. 2011;26(2):116-24.
9. Barbier C, Loubieres Y, Schmit C, Hayon J, Ricome JL, Jardin F, et al. Respiratory changes in inferior vena cava diameter are helpful in predicting fluid responsiveness in ventilated septic patients. Intensive Care Med. 2004;30(9):1740-6.
10. Anderson KL, Jenq KY, Fields JM, Panebianco NL, Dean AJ. Diagnosing heart failure among acutely dyspneic patients with cardiac, inferior vena cava, and lung ultrasonography. Am J Emerg Med. 2013;31(8):1208-14.
11. Gomez Betancourt M, Moreno-Montoya J, Barragan Gonzalez AM, Ovalle JC, Bustos Martinez YF. Learning process and improvement of point-of-care ultrasound technique for subxiphoid visualization of the inferior vena cava. Crit Ultrasound J. 2016;8(1):4.
12. Wallace DJ, Allison M, Stone MB. Inferior vena cava percentage collapse during respiration is affected by the sampling location: an ultrasound study in healthy volunteers. Acad Emerg Med. 2010;17(1):96-99.
13. Zhang Z, Xu X, Ye S, Xu L. Ultrasonographic measurement of the respiratory variation in the inferior vena cava diameter is predictive of fluid responsiveness in critically ill patients: systematic review and meta-analysis. Ultrasound Med Biol. 2014;40(5):845-53.
14. Gutierrez MA, Pilon PE, Lage SG, Kopel L, Carvalho RT, Furuie SS, et al. Automatic measurement of carotid diameter and wall thickness in ultrasound images. In: Computers in Cardiology, Memphis, TN, 22-25 September 2002.
15. Newey VR, Nassiri DK. Online artery diameter measurement in ultrasound images using artificial neural networks. Ultrasound Med Biol. 2002;28(2):209-16.
16. Cinthio M, Jansson T, Eriksson A, Ahlgren AR, Persson HW, Lindstrom K. Evaluation of an algorithm for arterial lumen diameter measurements by means of ultrasound. Med Biol Eng Comput. 2010;48(11):1133-40.
17. Biswas M, Kuppili V, Saba L, Edla DR, Suri HS, Sharma A, et al. Deep learning fully convolution network for lumen characterization in diabetic patients using carotid ultrasound: a tool for stroke risk. Med Biol Eng Comput. 2019;57(2):543-64.
18. Manterola HL, Lo Vercio L, Diaz A, Del Fresno M, Larrabide I. Validation of an open-source tool for measuring carotid lumen diameter and intima-media thickness. Ultrasound Med Biol. 2018;44(8):1873-81.
19. Mesin L, Pasquero P, Albani S, Porta M, Roatta S. Semi-automated tracking and continuous monitoring of inferior vena cava diameter in simulated and experimental ultrasound imaging. Ultrasound Med Biol. 2015;41(3):845-57.
20. Mesin L, Pasquero P, Roatta S. Tracking and monitoring pulsatility of a portion of inferior vena cava from ultrasound imaging in long axis. Ultrasound Med Biol. 2019;45(5):1338-43.
21. Bellows S, Smith J, Mcguire P, Smith A. Validation of a computerized technique for automatically tracking and measuring the inferior vena cava in ultrasound imagery. Stud Health Technol Inform. 2014;207:183-92.

22. Chen J, Li J, Ding X, Chang C, Wang X, Ta D. Automated identification and localization of the inferior vena cava using ultrasound: an animal study. Ultrason Imaging. 2018;40(4):232-44.
23. Konofagou E, Ophir J. A new elastographic method for estimation and imaging of lateral displacements, lateral strains, corrected axial strains and Poisson's ratios in tissues. Ultrasound Med Biol. 1998;24(8):1183-99.
24. Luo J, Konofagou EE. A fast normalized cross-correlation calculation method for motion estimation. IEEE Trans Ultrason Ferroelectr Freq Control. 2010;57(6):1347-57.